Journal of Science and Technology, Vol. 44, No. 4 (2026), pp 1 - 21
Kwame Nkrumah University of Science and Technology (KNUST)
https://dx.doi.org/10.4314/just.v44i4.1

DESIGN AND FABRICATION OF A RIGID HAND EXOSKELETON FOR STROKE REHABILITATION IN LOW-RESOURCE SETTINGS

***Ebenezer Martey, Benedict Opoku-Antwi, Frank K. A. Nyarko**
Mechanical Engineering Department, Kwame Nkrumah University of Science and Technology, Kuması, Ghana

***Corresponding Author: ebenezer.martey.36@gmail.com**

ABSTRACT
Upper limb impairments resulting from stroke significantly reduce hand functionality and limit the ability of affected individuals to perform activities of daily living (ADLs). Conventional stroke rehabilitation methods, primarily administered through physical therapy, face limitations related to accessibility, personalisation, and rehabilitation intensity. Hand exoskeleton devices have emerged as promising rehabilitation solutions capable of enhancing motor recovery through assisted and repetitive hand movements. This study presents the design, fabrication, and preliminary evaluation of a rigid robotic hand exoskeleton intended for stroke rehabilitation in low-resource settings. The methodology involved the study of the anatomy and biomechanics of the human hand, which informed the development of three initial design concepts. The concepts were evaluated based on engineering design requirements, including cost, performance, wearability, portability, and usability, after which the most suitable concept was selected for further development. The hand exoskeleton was fabricated using 3D printing with PLA as the main material, and the necessary kinematic analysis was performed to support the design process. Initial testing of the assembled device under donned and doffed conditions demonstrated controlled flexion and extension movements and showed that the device was able to provide 10 out of the intended 14 degrees of freedom during operation. However, limitations, including restricted range of motion and rigidity-related movement constraints, were observed. The findings demonstrate the feasibility of the proposed rigid hand exoskeleton as a rehabilitation assistance device while highlighting the need for further improvements in adaptability, flexibility, and joint actuation performance.

Keywords: Stroke rehabilitation, wearable devices, hand exoskeletons, exoskeleton design requirements, assistive technologies.

INTRODUCTION

Background

Stroke is a severe brain condition that has a high chance of death and long-term physical challenges (Benjamin *et al*., 2019). Stroke is more likely to occur at an older age but can happen at any time (Barthels and Das, 2020). Globally, according to the World Stroke Organisation (WSO), reported by Feigin *et al*. (2022), there are 12.2 million new strokes each year, with over 16% of all strokes occurring in people between 15 and 49 years of age, while 62% of all strokes occur in people under the age of 70 years. Certain health and lifestyle issues, such as diet, smoking, high blood pressure, and diabetes, can increase the likelihood of stroke occurrence. These factors often affect the cardiovascular system, and assessing cardiovascular health can help predict stroke risk (Benjamin *et al*., 2019).

Post-stroke patients often experience significant challenges in regaining functional independence, particularly in the upper limb. Reduced mobility and dexterity in the hand significantly inhibit the ability of affected individuals to perform daily activities, which leads to a reduced quality of life.

Conventional rehabilitation methods, such as physical therapy, have been effective over the years; however, there remains a gap in providing personalised interventions for hand function improvement. Commercial rehabilitation devices, which are currently being developed to address the limitations of conventional therapy, are often difficult to transport and install due to their weight, size, and complex setup requirements. As a result, these devices are typically limited to rehabilitation centres and are not widely accessible. They also require patients to travel to these centres, which introduces additional cost and time constraints. The need for a specialised and adaptable solution is therefore evident, necessitating the design and fabrication of a robotic hand exoskeleton that can be tailored to the specific needs of each stroke survivor.

In recent years, robotic exoskeletons have played a prominent role in rehabilitation therapies and have shown potential to improve the recovery of mobility and impaired motor functions compared to conventional therapies. These devices offer novel solutions for augmenting movement, providing targeted support, and facilitating motor recovery in individuals with neurological conditions. According to du Plessis *et al*., exoskeletons have been demonstrated by Staubli *et al*. and Lum *et al*. to enhance rehabilitation while reducing muscle strain and decreasing localised muscle activity. Robotic hand exoskeletons, in particular, have gained attention for their potential to restore hand function and improve upper limb mobility in stroke survivors.

Hand exoskeletons are external wearable devices equipped with electric, pneumatic, or hybrid actuation systems that enable controlled hand and joint movements with improved endurance and strength. These devices are typically designed to operate within the required range of motion for rehabilitation. The primary purpose of a hand exoskeleton device is to support the recovery and restoration of motor function in individuals with impaired hand movement. They help reduce fatigue, prevent further injury, and improve the efficiency of motor function recovery. In the context of stroke rehabilitation, hand exoskeletons provide controlled and personalised support to enhance the recovery of hand mobility and functionality, thereby addressing the specific rehabilitation needs of post-stroke patients.

To address these challenges, this study focuses on the design and fabrication of a robotic hand exoskeleton intended to provide controlled and personalised assistance for hand rehabilitation.

The lack of a tailored robotic exoskeleton solution for hand rehabilitation poses a significant challenge in optimising recovery outcomes for post-stroke patients, particularly in resource-limited settings.

Human Hand Anatomy

The human hand is a complex structure that combines anatomy and biomechanics to offer exceptional dexterity and precision (Chen *et al*., 2013). The hand has several degrees of freedom that enable movements such as flexion, extension, abduction, adduction, and circumduction (Wang *et al*., 2017). While individual finger movements are possible, most everyday hand actions involve coordinated movement of multiple fingers (Dupan *et al*., 2018). The hand is made up of bones, joints, ligaments, tendons, and muscles that work in unison to allow both fine motor and gross movements. There are 27 bones in the human hand, which are grouped into three main sections: the phalanges (the fingers), the metacarpus (the palm), and the wrist (the carpus) (Kehr and Graftiaux, 2017). The carpometacarpal (CMC), metacarpophalangeal (MCP), and interphalangeal (IP) joints support the bones to allow for specific hand motions (Jaworski & Karpiński, 2017). The thumb plays a pivotal role in the performance of grasping functions due to its unique anatomy and range of motion (Neumann & Bielefeld, 2003; Kivell, 2015). The types of grasps are categorised into precision, power, and hook grips, with each serving a specific function (Feix *et al*., 2016; Napier, 1956).

The understanding of the biomechanics of the human hand plays a vital role in informing the design of robotic, prosthetic, and rehabilitation systems.

State-of-The-Art: Hand Exoskeletons for Rehabilitation

A hand exoskeleton, according to du Plessis *et al*., is a wearable robotic device capable of assisting the fingers of the human hand to complete their range of motion (ROM), amplify power, rehabilitate impaired hands, or provide haptic feedback for virtual or teleoperation applications. With the help of hand exoskeleton devices, patients can engage in independent rehabilitative exercises, either at home or in clinical settings. These devices contribute to the accessibility, affordability, and effectiveness of physical therapy, thereby increasing the potential for improved rehabilitation outcomes (Polygerinos *et al*., 2015).

Hand exoskeleton devices are typically classified based on specific criteria, mainly focusing on technical features such as performance specifications or design architecture. Commonly examined aspects include the availability and number of actuators or actuated degrees of freedom (DOFs), the number of actuated fingers, the types of movements permitted, the actuation technology, and the use of sensors. The work of du Plessis *et al*. classifies hand exoskeletons into two main categories: based on their purpose and based on their design type.

Throughout the years, each class of hand exoskeleton has established specific requirements to fulfil its intended function. Hand exoskeletons can also be grouped as active or passive systems. Active exoskeletons are equipped with motors or actuators that contribute to movement by providing assistance or resistance (Siran and Ribuan, 2021; Agarwal *et al*., 2017; Tang *et al*., 2013).

Passive exoskeletons, on the other hand, lack powered components such as motors and rely on mechanical elements, including springs, to provide support or reduce the load on the wearer (In *et al*., 2011; Li *et al*., 2020; Srivastava *et al*., 2022).

- **Based on purpose:** With regard to the intended use of the device, hand exoskeletons can be categorized as augmentative, haptic, rehabilitative, or assistive. Augmentative exoskeletons are designed to enhance and amplify the physical capabilities of the human body, while haptic exoskeletons provide tactile feedback or a sense of touch to the wearer. Rehabilitative exoskeletons are developed to aid individuals in their physical recovery after injury or illness, particularly by improving motor function (Meng *et al*., 2023; Yang *et al*., 2016). Assistive exoskeletons are designed to support and complement natural human movements (Chen *et al*., 2021; Tong *et al*., 2010; Haghshenas-Jaryani *et al*., 2020).
- **Based on design type or architecture:** After defining the purpose of the device, the architectural design of the hand exoskeleton must also be considered. Hand exoskeletons are generally categorised into three types: soft, rigid, and hybrid systems. Soft exoskeletons are flexible and compliant, allowing them to mimic the behaviour of biological muscles. They are typically actuated using pneumatic or hydraulic systems (Hu *et al*., 2020; Kadowaki *et al*., 2011; Meng *et al*., 2023; Polygerinos *et al*., 2015). Rigid exoskeletons employ solid mechanical structures and are commonly actuated using electric motors. These systems utilise stiff links and joints to transmit forces or torques from actuators to the required joints, enabling precise control and assistance of hand movements (Tong *et al*., 2010; Rahman and Al-Jumaily, 2012; Moreno-SanJuan *et al*., 2021). Hybrid exoskeletons combine elements of both soft and rigid systems, offering a balance between strength, compliance, and user comfort. These systems are suitable for a wide range of applications, including rehabilitation, assistance, and augmentation (Rose & O'Malley, 2019; Vertongen & Kamper, 2020; Wang *et al*., 2019).

Despite the wide range of hand exoskeleton designs reported in the literature, several limitations remain. Many existing systems are either complex, expensive, or reliant on soft or hybrid actuation mechanisms that may not be easily adaptable for use in resource-limited environments. In addition, some designs prioritise high degrees of freedom and advanced control strategies at the expense of structural simplicity, manufacturability, and accessibility. These challenges highlight the need for alternative design approaches that balance functionality with simplicity and cost-effectiveness.

To address these limitations, this study presents the design and fabrication of a rigid hand exoskeleton prototype developed using 3D-printed components. The proposed system employs a mechanical linkage-based force transmission mechanism driven by linear actuators to provide controlled finger movement. The design emphasises mechanical robustness, precise motion control, and ease of fabrication, while maintaining structural simplicity. Unlike many existing systems that rely on soft or highly complex actuation strategies, this approach prioritises durability, manufacturability, and accessibility, making it more suitable for deployment in low-resource settings. The study contributes by presenting a proof-of-concept design and evaluating its functional performance through preliminary testing, thereby providing a foundation for further development and clinical validation.

METHODOLOGY

This section outlines the design methodology used to achieve the objectives of this study. It presents the key engineering requirements and design specifications that guided the concept generation process. The final design concept was selected through a structured evaluation using a design matrix, which considered factors such as functionality, manufacturability, and cost-effectiveness. Each potential design concept was assessed against these criteria, and the concept with the highest overall score was selected.

Engineering Requirements and Design Specification

The engineering requirements and design specifications adopted in this study are based on the general design flowchart for robotic hand exoskeleton devices proposed by Achilli *et al*. (2023). This framework provides a structured approach for the development of hand rehabilitation exoskeletons. The essential requirements considered are outlined as follows:

1. **Purpose of the device:** The device proposed in this study is intended for stroke rehabilitation, with a focus on addressing upper limb impairment. Its functionality is aimed at supporting hand movement recovery during rehabilitation exercises.
2. **Functional requirements:** The functional requirements define the degrees of freedom (DoFs) to be actuated, the required range of motion (ROM), the forces to be generated, and the type of rehabilitative exercises supported by the device. The proposed device is designed to actuate all 14 joints of the hand at allowable joint angles. It must be capable of delivering sufficient force at the fingertips to support grasping, while enabling flexion and extension movements during rehabilitation training. These movements are intended to replicate fundamental rehabilitative hand exercises required for motor recovery and functional grasp rehabilitation.
3. Interactive experience requirements: These requirements include the wearability, usability, and portability of the proposed device.
    - **Wearability:** This includes considerations of comfort, size, weight, and safety. The device should minimize user encumbrance during operation and utilise materials that are safe for skin contact. Actuators are positioned on the dorsal side of the hand to reduce obstruction of natural motion. The system must remain lightweight and should not significantly alter the natural movement of the hand. In addition, fail-safe mechanisms must be incorporated to ensure user safety.
    - **Usability:** The device should be simple to operate and capable of performing required rehabilitation tasks within reasonable timeframes.
    - **Portability:** The device should be easy to wear independently and should not restrict the user's general movement during use.
4. Actuation technology: The selection of actuation technology (electric, pneumatic, or hydraulic) must align with the functional and design requirements. The specific actuator type, such as electric motors, gear trains, or linear actuators, is chosen based on performance, control, and integration considerations.
5. **Exoskeleton design:** The structural design of the exoskeleton must ensure effective force transmission while maintaining alignment with the natural biomechanics of the human hand. The device components are to be fabricated using 3D printing techniques and should allow for ease of assembly and maintenance.

The structural configuration must also ensure stable load transfer across the linkage system during actuation while maintaining alignment with finger joint motion.

6. **Affordability:** The device is intended for use in low-resource settings; therefore, manufacturing and material costs must be minimised. The design should also require minimal maintenance to ensure long-term usability.
7. **Environmental friendliness:** The materials and fabrication processes used in the device should comply with relevant environmental standards and sustainability considerations.

Concept Selection and Final Design

Concept Description

- **Concept One:** Concept One is a rigid hand exoskeleton designed for rehabilitation and intended to be fabricated using PLA or ABS. It utilises a mechanical linkage system for force transmission and is designed to provide 14 degrees of freedom (DOFs) for hand motion: 12 DOFs for the DIP, PIP, and MCP joints of the fingers, and 2 DOFs for the IP and MCP joints of the thumb. Key components of the device include a rigid exoskeleton structure, linear actuators for each finger, a microcontroller for actuator control, and Velcro straps for attachment to the hand. The device operates by transmitting force from the linear actuators through the mechanical linkages, thereby enabling flexion and extension movements that mimic natural hand joint motion.
- **Concept Two:** Concept Two incorporates flexible or bendable strips to assist finger movement during rehabilitation. The device is intended to be developed using PLA or ABS for the rigid frame and TPU or TPE for the flexible strips. Its key components include the exoskeleton structure, linear actuators, a microcontroller, flexible strips, and Velcro straps for attachment. In this concept, force generated by the linear actuators is transmitted through mechanical links to the flexible strips, which in turn assist finger motion. Flexion and extension are primarily achieved at the MCP joints of the four fingers, while the thumb remains fixed.
- **Concept Three:** Concept Three is a rigid hand exoskeleton designed for rehabilitation and intended to be fabricated using PLA or ABS. The primary components include the exoskeleton framework, linear actuators, a microcontroller unit for control, and double-ring mechanisms with soft cushioning to enhance user comfort. Force is transmitted through mechanical linkages from the actuators to enable flexion and extension movements at the finger joints. The use of ring-based interfaces provides localized support and improves contact between the device and the fingers.

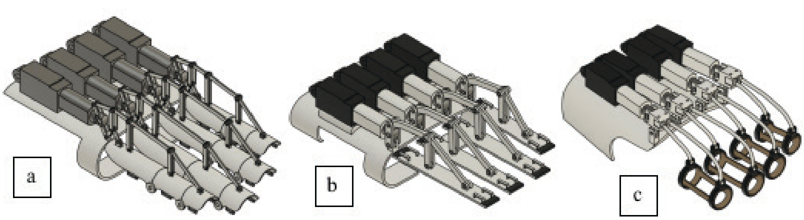

Figure 1: Conceptual designs; a. Concept 1, b. Concept 2, c. Concept 3

Final Design

The design concepts were evaluated based on criteria including cost, performance, wearability, portability, and usability. These criteria were used to assess the feasibility and effectiveness of each concept in meeting the functional and practical requirements of a hand exoskeleton for rehabilitation. Following this evaluation, Concept One was selected as the final design. This concept demonstrated strong alignment with the defined engineering requirements, particularly in terms of structural simplicity, effective force transmission, and the ability to actuate multiple joints of the hand. Its design also supports manufacturability using 3D printing techniques while maintaining a balance between functionality and usability, making it suitable for further development and evaluation. The rigid linkage-based configuration also provided improved joint support and more predictable force transmission compared to the alternative concepts considered.

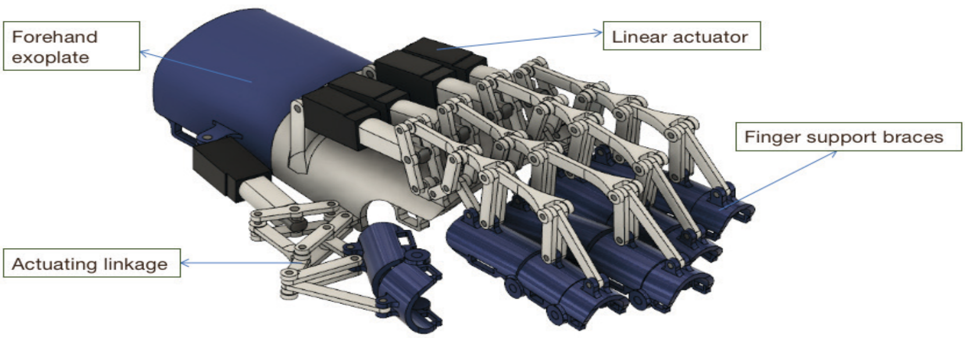

Figure 2: Final design of the hand exoskeleton

Design Analysis

Kinematic Analysis

The kinematic analysis of the proposed hand exoskeleton was carried out to study the motion behaviour of the linkage mechanism and to guide the selection of suitable linkage dimensions for effective force transmission from the linear actuators to the finger joints. The analysis focused on ensuring that the interconnected linkage system could support the flexion and extension movements required for rehabilitation while accommodating the allowable range of motion (ROM) of the finger joints.

A loop-based position analysis and preliminary kinematic synthesis approach involving interconnected four-bar and three-bar linkage systems was adopted to evaluate the motion relationships within the mechanism. Due to the similarity in motion behaviour across the fingers, the index finger mechanism was selected as the representative model for the analysis. The linkage system was assumed to operate as a planar mechanism with rigid links connected through revolute joints.

Firstly, the mobility of the linkage system was determined using the Kutzbach mobility criterion for planar linkages to establish the number of independent degrees of freedom possessed by the mechanism. The mobility of a mechanism is the number of independent inputs, or degrees of freedom, required to produce motion within the linkage system. The mobility equation is given as:

$$\text{Mobility (M)} = 3(n-1) - \sum_{i=1}^{J} (3 - f_i)$$

n = number of links = 11

j = number of joints = 14

 = degree of freedom of joint = 1 (for revolute joints)

Substituting these values into the mobility equation produced a mobility value of:

M = 3(11-1) - 14(3-1) = 2

This indicates that the mechanism has two independent degrees of freedom, implying that the motion of the linkage system can be controlled through two independent input parameters during operation.

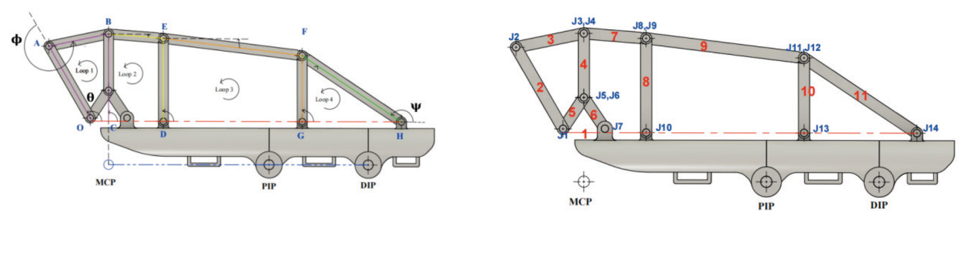

Figure 3: a. Defined number of links and joints of the linkage design, b. Angles and specified loops of the linkage design

Following the mobility analysis, the index finger mechanism was decomposed into a series of interconnected closed-loop systems to simplify the kinematic analysis. The mechanism consists of interconnected links through which motion is transmitted from the actuator-driven proximal section of the finger toward the distal joints during flexion and extension. The index finger assembly was divided into four loops consisting of three four-bar linkage loops and one three-bar linkage loop, as illustrated in Figure 3b.

This decomposition allowed the motion relationships between adjacent links to be analysed progressively, since the output motion of one loop directly influences the input motion of the succeeding loop. The shared links between adjacent loops therefore act as motion-transmitting elements across the mechanism. For each loop, the corresponding input, coupler, and output link angles, together with the governing geometric constraints, were defined to evaluate the linkage motion behaviour. The resulting relationships were used to guide the estimation and selection of suitable linkage dimensions capable of supporting the required rehabilitation movement of the finger joints.

For Loop 1, the coordinates of the linkage points and the associated link lengths were defined in terms of their $\begin{Bmatrix} x \\ y \end{Bmatrix}$ positional components, as illustrated in Figure 4. The angular relationships within the loop were represented using the following parameters:

θ = input angle

Φ = coupler angle ψ = output angle

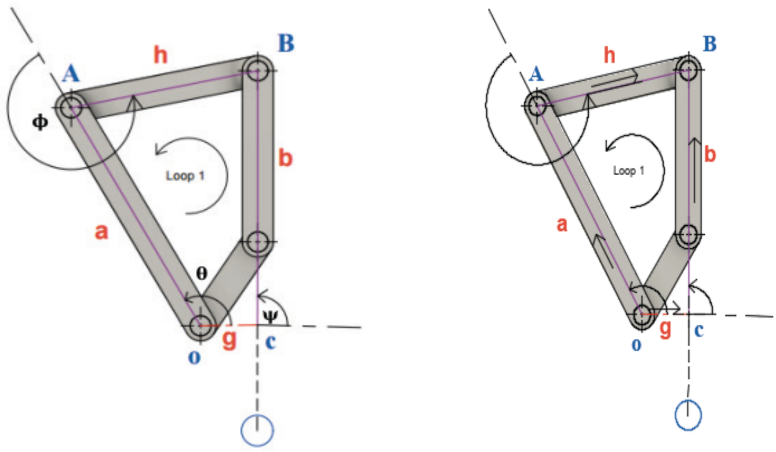

Figure 4: a. Angle specification of Loop 1, b. Vector representation of Loop 1

The input angle θ represents the angular displacement introduced into the linkage system through the actuator-driven input link, while the coupler angle θ and output angle ψ describe the motion transfer across the interconnected links of the mechanism. These angular relationships were used to establish the geometric constraints governing the motion of the linkage during finger flexion and extension. The vector positions of the joints within Loop 1 (OABC) were expressed relative to the origin point O using trigonometric relationships involving the sine and cosine components of the link angles. This allowed the positional relationships between the interconnected links to be represented geometrically during motion.

$$\vec{O} = \begin{Bmatrix} 0 \\ 0 \end{Bmatrix}, \vec{A} = \begin{Bmatrix} a.cos\theta \\ a.sin\theta \end{Bmatrix}, \vec{C} = \begin{Bmatrix} g \\ 0 \end{Bmatrix}$$

$$\vec{B} = \overrightarrow{OC} + \overrightarrow{AC} = \begin{Bmatrix} a.cos\theta \\ a.sin\theta \end{Bmatrix} + \begin{Bmatrix} h.cos(\theta+\phi) \\ h.sin(\theta+\phi) \end{Bmatrix} \text{ or } \overrightarrow{OC} + \overrightarrow{AC} = \begin{Bmatrix} g \\ 0 \end{Bmatrix} + \begin{Bmatrix} b.cos(\psi) \\ b.sin(\psi) \end{Bmatrix}$$

The relationship between the input angle, , of the driving link and the output angle, θ , of the driven link was established from the geometric constraint that the distance between points A and B remains constant throughout the motion of the mechanism, such that:

,b = |B - A| = constant.

Equations (1) – (7) were therefore derived to define the positional relationships between the links and to obtain the angular relationship governing the motion transfer within the four-bar linkage loop. The resulting expressions were used to estimate feasible linkage behaviour capable of supporting the required finger flexion and extension movements.

The constraint equation is given as:

$$(B - A)\cdot(B - A) - h^2 = 0 \qquad \textbf{eqn1}$$

The coordinates of A and B are given as, substitute (2) into (1), which gives:

$$A = \begin{Bmatrix} a.cos\theta \\ a.sin\theta \end{Bmatrix}, B = \begin{Bmatrix} g+cos(\psi) \\ b.sin(\psi) \end{Bmatrix} \quad \textbf{eqn 2}$$

$$\left(\begin{Bmatrix} g+bcos(\psi) \\ b.sin(\psi) \end{Bmatrix} - \begin{Bmatrix} a.cos\theta \\ a.sin\theta \end{Bmatrix}\right) \cdot \left(\begin{Bmatrix} g+bcos(\psi) \\ b.sin(\psi) \end{Bmatrix} - \begin{Bmatrix} a.cos\theta \\ a.sin\theta \end{Bmatrix}\right) = h^2 \quad \textbf{eqn 3}$$

$$(g + bcos(\psi) - a.cos\theta)^2 + (b.sin(\psi) - a.sin\theta)^2 = h^2$$

$$g^2 + b^2cos^2(\psi) + a^2cos^2\theta + 2gbcos(\psi) - 2gacos\theta - 2abcos(\psi)cos\theta + b^2sin^2(\psi) + a^2sin^2\theta - 2absin(\psi)sin\theta = h^2 \quad \textbf{eqn4}$$

$$(2b(g - acos\theta))cos(\psi) + (-2absin\theta)sin(\psi) = 2gacos\theta + h^2 - g^2 - a^2 - b^2$$

where,

$$A(\theta) = 2b(g - acos\theta)$$
$$B(\theta) = -2absin\theta)$$
$$C(\theta) = 2gacos\theta + h^2 - g^2 - a^2 - b^2$$

which leads to,

$$A(\theta)cos(\psi) + B(\theta)sin(\psi) = C(\theta) \quad \textbf{eqn 5}$$

is divide by

$$\sqrt{A^2(\theta) + B^2(\theta)}$$

which gives,

$$\frac{A(\theta)}{\sqrt{A^2(\theta)+B^2(\theta)}}cos(\psi) + \frac{B(\theta)}{\sqrt{A^2(\theta)+B^2(\theta)}}sin(\psi) = \frac{C(\theta)}{\sqrt{A^2(\theta)+B^2(\theta)}} \quad \textbf{eqn 6}$$

this allows the introduction of angle δ, such

that, and which gives,

$$\cos\delta = \frac{A(\theta)}{\sqrt{A^2(\theta)+B^2(\theta)}} \text{ and } \sin\delta = \frac{B(\theta)}{\sqrt{A^2(\theta)+B^2(\theta)}}$$

which gives,

$$\cos\delta cos(\psi) + sin\,\delta\sin(\psi) = \frac{C(\theta)}{\sqrt{A^2(\theta)+B^2(\theta)}}$$

which according to trigonometry, gives,

$$cos(\psi - \delta) = \frac{C(\theta)}{\sqrt{A^2(\theta)+B^2(\theta)}} \text{ and hence, } (\psi - \delta)$$

Also,

$$\text{also, } \delta = \frac{\sin\delta}{\cos\delta} = \arctan\frac{A(\theta)}{B(\theta)}$$

therefore,

$$\psi = \arctan\frac{A(\theta)}{B(\theta)} \pm arccos\frac{C(\theta)}{\sqrt{A^2(\theta)+B^2(\theta)}} \qquad \textbf{eqn 7}$$

The output angle (ψ) is dependent on the input angle (θ) and the geometric constraint,

$$A^2(\theta) + B^2(\theta) - C^2(\theta) \geq 0,$$

must be satisfied for a valid solution to exist. If this condition is not satisfied for a specified crank angle, the linkage configuration cannot be assembled or operated within the intended motion range. The coupler angle (ϕ) was measured relative to point A, referenced from the segment $\overrightarrow{OA}$, so (θ+ϕ) defines the orientation of the coupler link with respect to the global x-axis. The position of B was subsequently expressed in terms of the coupler angle from the Loop 1 vector relationship:

$$\overrightarrow{OA} + \overrightarrow{AB} = \overrightarrow{OC} + \overrightarrow{CB}$$

Equations (8) and (9) were derived from the vector loop relationship to establish the positional relationship governing the coupler link motion within the mechanism.

$$\begin{Bmatrix} a.cos\theta \\ a.sin\theta \end{Bmatrix} + \begin{Bmatrix} h.cos(\theta+\phi) \\ h.sin(\theta+\phi) \end{Bmatrix} = \begin{Bmatrix} g \\ 0 \end{Bmatrix} + \begin{Bmatrix} b.cos(\psi) \\ b.sin(\psi) \end{Bmatrix}$$

$$\begin{Bmatrix} a.cos\theta+h.cos(\theta+\phi) \\ a.sin\theta+h.sin(\theta+\phi) \end{Bmatrix} = \begin{Bmatrix} g+b.cos(\psi) \\ b.sin(\psi) \end{Bmatrix}$$

$$a.cos\theta + h.cos(\theta+\phi) = g + b.cos(\psi) \qquad \textbf{eqn 8}$$

$$a.sin\theta + h.sin(\theta+\phi) = b.sin(\psi) \qquad \textbf{eqn 9}$$

$$\frac{h.sin(\theta+\phi)}{h.cos(\theta+\phi)} = \frac{b.sin(\psi)-a.sin\theta}{g+b.cos(\psi)-a.cos\theta}$$

$$\tan(\theta+\phi) = \frac{\sin(\theta+\phi)}{\cos(\theta+\phi)} = \frac{b.sin(\psi)-a.sin\theta}{g+b.cos(\psi)-a.cos\theta}$$

$$(\theta+\phi) = arctan(\frac{b.sin(\psi)-a.sin\theta}{g+b.cos(\psi)-a.cos\theta})$$

$$\phi = arctan(\frac{b.sin(\psi)-a.sin\theta}{g+b.cos(\psi)-a.cos\theta}) - \theta$$

The resulting expression for the coupler angle was then used together with the previously obtained output-angle relationship to evaluate the motion behaviour of the linkage system during finger actuation.

The Freudenstein method was adopted as a geometric synthesis approach to estimate suitable linkage dimensions for the four-bar loops in the mechanism. The method establishes a functional relationship between the input angle (θ) and output angle (ψ) of a four-bar linkage system and is commonly applied in mechanism synthesis to evaluate linkage behaviour for specified motion conditions. In function generation with this method, the goal is to determine the link lengths that yield a (ψ - θ) relationship matching a desired design equation. In this study, this method helps guide the selection of feasible link dimensions capable of supporting the desired flexion and extension movements of the finger joints. For Loop 1, the vector loop equation was expressed as:

$$\overrightarrow{OA} + \overrightarrow{AB} = \overrightarrow{OC} + \overrightarrow{CB}$$

$$\begin{Bmatrix} a.cos\theta \\ a.sin\theta \end{Bmatrix} + \begin{Bmatrix} h.cos(\theta+\phi) \\ h.sin(\theta+\phi) \end{Bmatrix} = \begin{Bmatrix} g \\ 0 \end{Bmatrix} + \begin{Bmatrix} b.cos(\psi) \\ b.sin(\psi) \end{Bmatrix}$$

where a, b, h, and g represent the linkage lengths within the four-bar configuration.

To simplify the synthesis process, the linkage problem was treated as a scaling problem since the angular relationship between the input and output links remains unchanged when all link lengths are scaled proportionally. Consequently, one of the links was assigned a normalised value (for example, g = 1) during the analysis, after which the dimensions could be scaled to practical values for the physical mechanism. Using the relationships obtained from Equations (8) and (9), Equations (10) and (11) were derived to relate the unknown linkage dimensions and angular parameters. The equations were subsequently manipulated by squaring and summing the expressions to eliminate the coupler angle (ϕ), resulting in an expression for h^2, given in Equation (12).

$$a.cos\theta + h.cos(\theta+\phi) = 1 + b.cos(\psi)$$
$$a.sin\theta + h.sin(\theta+\phi) = b.sin(\psi)$$

$$h.cos(\theta+\phi) = 1 + b.cos(\psi) - a.cos\theta \quad \textbf{eqn 10}$$

$$h.sin(\theta+\phi) = b.sin(\psi) - a.sin\theta \quad \textbf{eqn 11}$$

Which leaves four unknowns a, b, h and ϕ. Both equations are squared and summed to eliminate ϕ .

$$(h.cos(\theta+\phi))^2 = (1 + b.cos(\psi) - a.cos\theta)^2$$
$$(h.sin(\theta+\phi))^2 = (b.sin(\psi) - a.sin\theta)^2$$
$$h^2 = 1 + b^2cos^2(\psi) + a^2cos^2(\theta) - 2acos(\theta) + 2bcos(\psi) - 2abcos(\psi)cos(\theta) + b^2sin^2(\psi) + a^2sin^2(\theta) - 2absin(\psi)sin(\theta)$$
$$h^2 - 1 - b^2 - a^2 = -2acos(\theta) + 2bcos(\psi) - 2abcos(\psi)cos(\theta) - 2absin(\psi)sin(\theta)$$

After simplifying, the desired design equation is obtained as:

$$h^2 = 1 + b^2 + a^2 - 2acos(\theta_i) + 2bcos(\psi_i) - 2abcos(\psi_i - \theta_i) \quad \textbf{eqn 12}$$

The resulting angular relationships between $\psi$and θ were then used together with geometric estimation and trigonometric calculations to guide the selection of feasible linkage dimensions for the mechanism. The same analytical approach was subsequently extended to the remaining loops of the index finger mechanism and later adapted for the remaining fingers of the hand exoskeleton.

Finite Element Analysis

Static finite element analysis (FEA) was performed on the proposed design using the Product Simulation function in Autodesk Fusion 360. The analysis was conducted on the three major sections of the hand exoskeleton: the forehand plate, the finger support braces, and the mechanical linkages.

Material properties corresponding to ABS were used during the simulation analysis. A static loading condition was adopted to evaluate the structural response of the assembled components during operation. To evaluate the structural integrity of the assembled device, forces were applied at critical points within the mechanism where load transfer was expected during operation. These locations included the linkage connection points, fastening interfaces between links, and the attachment regions between the linkages, finger support braces, and the forehand exoplate. The applied loading conditions were intended to simulate the forces transmitted through the mechanism during finger actuation and rehabilitation movement. Appropriate boundary constraints were applied at fixed support regions of the structure to simulate operational conditions during rehabilitation exercises.

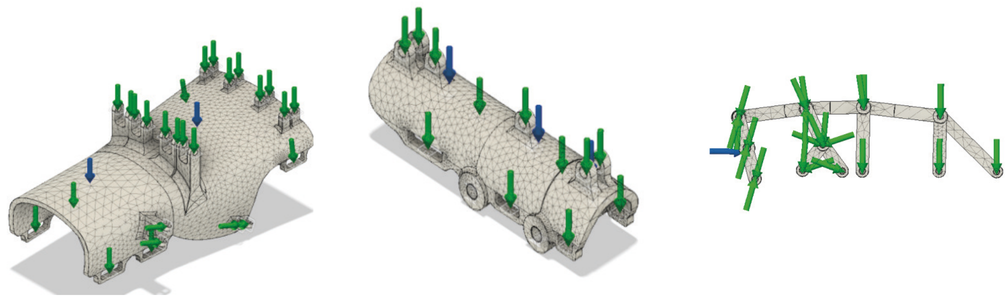

Figure 5: Loading and meshing for; a. Forehand exoplate with force and pressure loading and meshing, b. Finger support braces, c. Linkages

The analysis was performed to assess the ability of the 3D-printed components to withstand operational loading without structural failure. Simulation outputs including the factor of safety, von Mises stress, displacement, and equivalent stress distribution were evaluated for all major components of the design. The obtained results indicated that the stresses and displacements remained within acceptable operating limits for the selected material and loading conditions. The analysis therefore provided preliminary validation of the structural integrity and load-bearing capability of the proposed 3D-printed design.

Actuation system and control strategy

The control system for the proposed device is illustrated in the schematic diagram below. The device is actuated using five micro linear actuators, with each actuator assigned to a corresponding finger mechanism.

The micro linear actuators are controlled using three L298N H-bridge motor drivers, which receive control instructions from an Arduino UNO R3 microcontroller.

The actuation system enables controlled flexion and extension of the finger mechanisms through the mechanical linkage arrangement. Independent actuation of each finger mechanism allows controlled rehabilitation movement and improves flexibility during training exercises. Force sensors are integrated into the device to measure the force generated at the fingertips during actuation. These sensors provide feedback that can be used to monitor interaction forces during rehabilitation exercises and assist in evaluating the performance of the device.

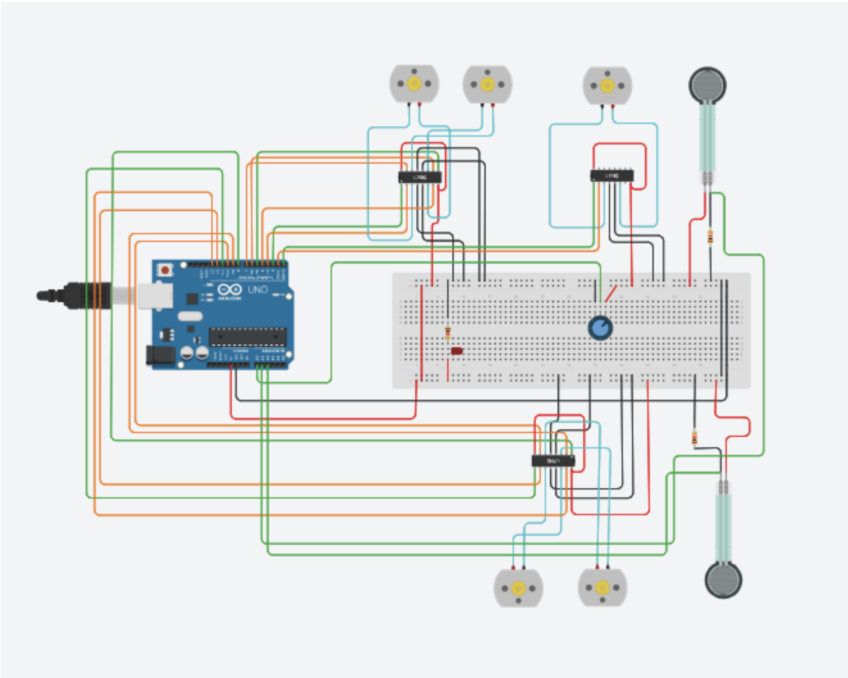

Figure 6: Schematic diagram of the Arduino-based control system of the hand exoskeleton device.

RESULTS AND DISCUSSION

Fabrication Results

The fabrication process of the hand exoskeleton prototype was divided into two main phases: the rapid prototyping phase and the assembly phase. The rapid prototyping phase involved the fabrication of the forehand exoplate, finger support braces, and linkage components using 3D printing techniques, while the assembly phase focused on integrating the mechanical and electronic subsystems of the device. The assembly process involved connecting the printed structural components together with the electronic components, including the micro linear actuators, motor drivers, and Arduino-based control system required for device operation.

The fabricated components were assembled successfully with no significant fitting challenges observed during integration. This was largely attributed to the use of precise dimensional measurements of the individual phalanges during the design stage.

Anthropometric hand data was initially considered for the dimensional design of the device; however, significant variation in hand dimensions among individuals made the use of generalised average measurements less suitable for achieving an accurate fit. As a result, the design approach prioritised direct dimensional consideration of the intended hand structure to improve alignment between the device and finger joints.

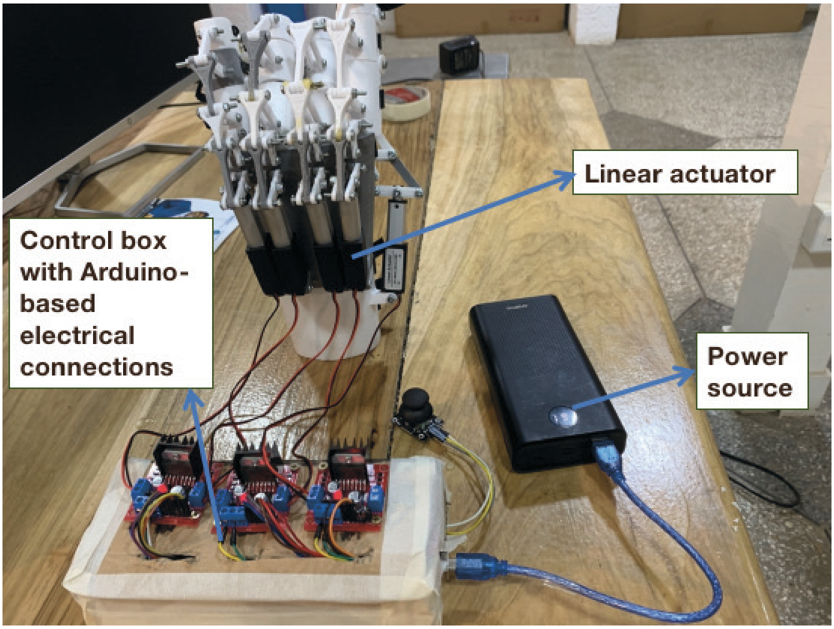

Figure 7: Final assembly setup of the proposed rigid hand exoskeleton prototype

Following assembly, the prototype demonstrated the intended flexion and extension movements through the mechanical linkage system. Due to the rigid structural configuration of the device, the motion of the individual phalanges exhibited limited flexibility compared to soft exoskeleton systems. The rigid architecture also introduced some restrictions to natural hand and finger movement during operation. However, this structural rigidity provided stable support and maintained finger extension during operation, which may be beneficial in rehabilitation scenarios involving patients with limited voluntary hand control following stroke. These observations were further reflected during functional testing, where limitations in distal joint actuation and range of motion were observed under donned conditions. The fabricated prototype demonstrated the feasibility of the proposed rigid linkage-based design and confirmed the integration capability of the mechanical and electronic subsystems for rehabilitation-oriented hand movement assistance.

Testing and Evaluation

Initial tests were carried out on the assembled device to ascertain its basic functionality after integrating the mechanical components and electrical connections. The tests were relevant to validate whether the device could actuate the intended degrees of freedom and produce flexion and extension movements at the finger joints. The flexion and extension motions of the hand exoskeleton were controlled using a joystick programmed through the Arduino control system. The device performs a flexing motion when the joystick is moved upward and performs an extension motion when the joystick is moved downward. The experiments carried out on the device included a series of flexion and extension tests with the device doffed, that is, without a subject, and donned on the hand of a healthy subject.

The actuation system consisted of 12 V micro linear actuators with a 30 mm stroke length and a rated force capacity of 60 N. These actuators transmitted motion to the finger mechanisms through the mechanical linkage system. The tests therefore focused on confirming joint actuation, linkage response, and the ability of the device to support finger flexion and extension under both free and worn conditions.

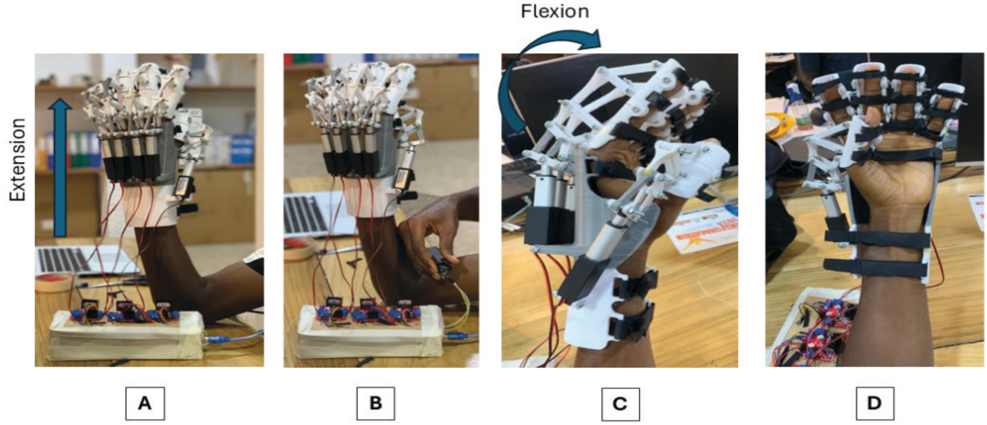

Figure 8: Flexion testing of the rigid hand exoskeleton under donned conditions showing actuator-driven finger motion through the linkage system, a. Extension, b. Flexion backside view, c. Flexion side view, d. Flexion frontside view

The test results from the doffed and donned experiments of the exoskeleton have been presented in Table 1, with '-' representing no observable actuation movement in the joints and '+' representing observable actuation movement in the joints. From the table, it can be noticed that there was no actuation in the IP joint of the thumb and the DIP and PIP joints of the remaining fingers when the device was tested in the doffed mode, that is, when the device was not worn. However, when the device was donned and tested on the hand of the healthy subject, no observable actuation was noticed in the DIP joints of the four remaining fingers. This implies that the fabricated hand exoskeleton device was able to provide 10 actuated degrees of freedom out of the intended 14 degrees of freedom when worn by the user, representing approximately 71.4% of the intended joint actuation. The device also provided a limited range of motion to the joints, which marginally fell below the maximum allowable anatomical range of motion of the finger joints.

Table 1: Qualitative flexion and extension actuation results of the hand exoskeleton under doffed and donned conditions

Test mode/ Finger and Joint	Thumb		Index			Middle			Ring			Little		
	IP	MCP	DIP	PIP	MCP	DIP	PIP	MCP	DIP	PIP	MCP	DIP	PIP	MCP
Doffed	-	+	-	-	+	-	-	+	-	-	+	-	-	+
Donned	+	+	-	+	+	-	+	+	-	+	+	-	+	+

(+) indicates observable actuation movement at the joint, while (-) indicates no observable actuation movement during testing.

The reduced actuation of the DIP joints may be attributed to the rigidity of the mechanical linkage system, joint alignment constraints, and resistance introduced when the device was worn on the hand. The observed reduction in distal joint actuation under worn conditions further highlights the influence of rigid linkage constraints and joint alignment challenges on the overall rehabilitation performance of the device. Although the prototype did not achieve the full intended joint actuation, the tests confirmed that the assembled device could perform controlled flexion and extension movements and demonstrated the preliminary functionality of the rigid linkage-based exoskeleton design. Further quantitative testing using joint-angle measurement tools, force sensors, and repeated actuation cycles will be required to characterize ROM, actuation speed, torque transmission, durability, and repeatability more accurately.

Limitations and Challenges of Current Prototype

Several limitations and challenges were encountered during the design, fabrication, and assembly stages of the hand exoskeleton prototype. These limitations influenced the overall functionality and operational performance of the device. The most significant challenges identified include the following:

i. Material limitations: The primary material available for fabrication of the 3D-printed components was PLA. Although suitable for rapid prototyping, the rigidity and brittle nature of PLA limited the durability of thinner structural sections, resulting in occasional component breakage during handling and assembly. The use of alternative materials such as ABS could potentially improve structural resilience and reduce brittleness.

ii. Structural rigidity and movement restriction: The assembled prototype exhibited a rigid structural configuration that limited the natural movement of the hand during operation. While the rigid architecture improved structural support and force transmission, it also constrained free hand and finger movement compared to more compliant soft exoskeleton systems.

iii. Limited joint actuation and range of motion: The prototype was unable to achieve all the intended degrees of freedom and the full required range of motion of the finger joints. This limitation was primarily associated with the rigidity of the linkage mechanism and alignment constraints during operation, particularly under donned conditions.

Addressing these limitations through improved material selection, enhanced linkage optimization, and refined joint alignment strategies could improve the overall functionality, flexibility, and rehabilitation effectiveness of future iterations of the device.

CONCLUSION

This study presented the design, fabrication, and preliminary evaluation of a rigid hand exoskeleton intended for post-stroke rehabilitation in low-resource settings. The device was developed based on the biomechanics and functional requirements of the human hand, with emphasis placed on structural simplicity, manufacturability, and rehabilitation-oriented motion assistance. A rigid linkage-based mechanism actuated using micro linear actuators was proposed and fabricated using 3D printing techniques.

Functional testing of the assembled prototype demonstrated controlled flexion and extension movements under both donned and doffed conditions. The device was able to actuate 10 out of the intended 14 degrees of freedom during worn operation, demonstrating the feasibility of the proposed rehabilitation concept. However, limitations, including reduced distal joint actuation, restricted range of motion, and rigidity-related movement constraints, were observed during testing. Despite these limitations, the study demonstrates the potential of rigid linkage-based hand exoskeleton systems as accessible rehabilitation devices for stroke patients, particularly in resource-constrained environments. Future work will focus on improving joint actuation performance, enhancing user comfort and flexibility, optimising linkage alignment, and integrating more advanced control and sensing strategies to improve rehabilitation effectiveness and overall device functionality.

CONFLICT OF INTEREST

The authors of this manuscript declare that there is no conflict of interest regarding the publication of this paper. The research was conducted independently, and the results presented reflect the findings and views of the authors without any influence from external parties. The authors received no financial support for the research, authorship, and/or publication of this manuscript.

If any potential conflict of interest arises in the future, the authors commit to promptly disclosing it to the relevant parties.

REFERENCES

Achilli, G.M., Amici, C., Dragusanu, M., Gobbo, M., Logozzo, S., Malvezzi, M., Tiboni, M., Valigi, M.C. Soft, Rigid, and Hybrid Robotic Exoskeletons for Hand Rehabilitation: Roadmap with Impairment-Oriented Rationale for Devices Design and Selection. Appl. Sci. 2023, 13, 11287. https://doi.org/10.3390/app132011287

Agarwal, P., Yun, Y., Fox, J., Madden, K., & Deshpande, A. D. (2017). Design, control, and testing of a thumb exoskeleton with series elastic actuation. The International Journal of Robotics Research, 36(3), 355–375. https://doi.org/10.1177/0278364917694428

Barthels, D., & Das, H. (2020). Current advances in ischemic stroke research and therapies. Biochimica Et Biophysica Acta (BBA) - Molecular Basis of Disease, 1866(4), 165260. https://doi.org/10.1016/j.bbadis.2018.09.012

Benjamin, E. J., Muntner, P., Alonso, A., Bittencourt, M. S., Callaway, C. W., Carson, A. P., Chamberlain, A. M., Chang, A. R., Cheng, S., Das, S. R., Delling, F. N., Djousse, L., Elkind, M. S., Ferguson, J. F., Fornage, M., Jordan, L. C., Khan, S. S., Kissela, B. M., Knutson, K. L., Virani, S. S. (2019). Heart Disease and Stroke Statistics—2019 Update: A Report From the American Heart Association. Circulation, 139(10). https://doi.org/10.1161/cir.0000000000000659

Chen Chen, F., Appendino, S., Battezzato, A., Favetto, A., Mousavi, M., & Pescarmona, F. (2013). Constraint Study for a Hand Exoskeleton: Human Hand Kinematics and Dynamics. Journal of Robotics, 2013, 1–17. https://doi.org/10.1155/2013/910961

Chen, Y., Yang, Z., & Wen, Y. (2021a). A Soft Exoskeleton Glove for Hand Bilateral Training via Surface EMG. Sensors, 21(2), 578. https://doi.org/10.3390/s21020578

du Plessis, T., Djouani, K., & Oosthuizen, C. (2021, March 3). A Review of Active Hand Exoskeletons for Rehabilitation and Assistance. Robotics, 10(1), 40. https://doi.org/10.3390/robotics10010040

Dupan, S. S., Stegeman, D. F., & Maas, H. (2018, June). Distinct neural control of intrinsic and extrinsic muscles of the hand during single finger pressing. Human Movement Science, 59, 223–233. https://doi.org/10.1016/j.humov.2018.04.012

Feigin, V. L., Brainin, M., Norrving, B., Martins, S., Sacco, R. L., Hacke, W., Fisher, M., Pandian, J., & Lindsay, P. (2022, January). World Stroke Organization (WSO): Global Stroke Fact Sheet 2022. International Journal of Stroke, 17(1), 18–29. https://doi.org/10.1177/17474930211065917

Feix, T., Romero, J., Schmiedmayer, H. B., Dollar, A. M., & Kragic, D. (2016, February). The GRASP Taxonomy of Human Grasp Types. IEEE Transactions on Human-Machine Systems, 46(1), 66–77. https://doi.org/10.1109/thms.2015.2470657

Haghshenas-Jaryani, M., Patterson, R. M., Bugnariu, N., & Wijesundara, M. B. (2020, April). A pilot study on the design and validation of a hybrid exoskeleton robotic device for hand rehabilitation. Journal of Hand Therapy, 33(2), 198–208. https://doi.org/10.1016/j.jht.2020.03.024

Hu, D., Zhang, J., Yang, Y., Li, Q., Li, D., & Hong, J. (2020). A novel soft robotic glove with positive-negative pneumatic actuator for hand rehabilitation. IEEE/ASME International Conference on Advanced Intelligent Mechatronics, AIM, 2020-July, 1840–1847. https://doi.org/10.1109/AIM43001.2020.9158826

In, H., Cho, K. J., Kim, K., & Lee, B. (2011). Jointless structure and under-actuation mechanism for compact hand exoskeleton. https://doi.org/10.1109/icorr.2011.5975394

Jaworski, U., & Karpiński, R. (2017, June 30). BIOMECHANICS OF THE HUMAN HAND. Journal of Technology and Exploitation in Mechanical Engineering, 3(1), 28–33. https://doi.org/10.35784/jteme.536

Kadowaki, Y., Noritsugu, T., Takaiwa, M., Sasaki, D., & Kato, M. (2011). Development of Soft Power-Assist Glove and Control Based on Human Intent. Journal of Robotics and Mechatronics, 23(2), 281–291. https://doi.org/10.20965/jrm.2011.p0281

Kehr, P., & Graftiaux, A. G. (2017, June 13). B. Hirt, H. Seyhan, M. Wagner, R. Zumhasch: Hand and wrist anatomy and biomechanics: a comprehensive guide. European Journal of Orthopaedic Surgery & Traumatology, 27(7), 1029–1029. https://doi.org/10.1007/s00590-017-1991-z

Kivell, T. L. (2015, November 19). Evidence in hand: recent discoveries and the early evolution of human manual manipulation. Philosophical Transactions of the Royal

Society B: Biological Sciences, 370(1682), 20150105. https://doi.org/10.1098/rstb.2015.0105

Li, M., Wang, T., Zhuo, Y., He, B., Tao, T., Xie, J., & Xu, G. (2020, June). A soft robotic glove for hand rehabilitation training controlled by movements of the healthy hand. 2020 17th International Conference on Ubiquitous Robots (UR). https://doi.org/10.1109/ur49135.2020.9144753

Lum, P. S., Burgar, C. G., Shor, P. C., Majmundar, M., & Van der Loos, M. (2002, July). Robot-assisted movement training compared with conventional therapy techniques for the rehabilitation of upper-limb motor function after stroke. Archives of Physical Medicine and Rehabilitation, 83(7), 952–959. https://doi.org/10.1053/apmr.2001.33101

Meng, F., Liu, C., Li, Y., Hao, H., Li, Q., Lyu, C., Wang, Z., Ge, G., Yin, J., Ji, X., & Xiao, X. (2023). Personalized and Safe Soft Glove for Rehabilitation Training. Electronics, 12(11), 2531. https://doi.org/10.3390/electronics12112531

Moreno-SanJuan, V., Cisnal, A., Fraile, J. C., Pérez-Turiel, J., & De-La-Fuente, E. (2021). Design and characterization of a lightweight underactuated RACA hand exoskeleton for neurorehabilitation. Robotics and Autonomous Systems, 143, 103828. https://doi.org/10.1016/j.robot.2021.103828

Napier, J. R. (1956). THE PREHENSILE MOVEMENTS OF THE HUMAN HAND. The Journal of Bone and Joint Surgery. British

Volume, 38-B(4), 902–913. https://doi.org/10.1302/0301-620x.38b4.902

Neumann, D. A., & Bielefeld, T. (2003). The Carpometacarpal Joint of the Thumb: Stability, Deformity, and Therapeutic Intervention. Journal of Orthopaedic & Sports Physical Therapy, 33(7), 386–399. https://doi.org/10.2519/jospt.2003.33.7.386

Polygerinos, P., Wang, Z., Galloway, K. C., Wood, R. J., & Walsh, C. J. (2015). Soft robotic glove for combined assistance and at-home rehabilitation. Robotics and Autonomous Systems, 73, 135–143. https://doi.org/10.1016/j.robot.2014.08.014

Rahman, M. A., & Al-Jumaily, A. (2012). Design and Development of a Hand Exoskeleton for Rehabilitation Following Stroke. Procedia Engineering, 41, 1028–1034. https://doi.org/10.1016/j.proeng.2012.07.279

Rose, C. G., & O'Malley, M. K. (2019). Hybrid Rigid-Soft Hand Exoskeleton to Assist Functional Dexterity. IEEE Robotics and Automation Letters, 4(1), 73–80. https://doi.org/10.1109/lra.2018.2878931

Siran, A. A., & Ribuan, M. N. (2022). Design and Develop Motorized Soft Robotic Glove for Hand Rehabilitation. Evolution in Electrical and Electronic Engineering, 3(2), 781–792. Retrieved from https://publisher.uthm.edu.my/periodicals/index.php/eeee/article/view/6671

Srivastava, R., Singh, M., Gomes, G. D., Murray, N., & Devine, D. (2022). SM-EXO: Shape Memory alloy-based Hand EXOskeleton for Cobotic Application. 2022 31st IEEE International Conference on Robot and Human Interactive Communication (RO-MAN). https://doi.org/10.1109/ro-man53752.2022.9900776

Staubli, P., Nef, T., Klamroth-Marganska, V., & Riener, R. (2009, December). Effects of intensive arm training with the rehabilitation robot ARMin II in chronic stroke patients: four single-cases. Journal of NeuroEngineering and Rehabilitation, 6(1). https://doi.org/10.1186/1743-0003-6-46

Tang, T., Zhang, D., Xie, T., & Zhu, X. (2013). An exoskeleton system for hand rehabilitation driven by shape memory alloy. https://doi.org/10.1109/robio.2013.6739553

Tong, K. Y., Ho, S. K., Pang, P. M. K., Hu, X. L., Tam, W. K., Fung, K. L., Wei, X. J., Chen, P. N., & Chen, M. (2010). An intention driven hand functions task training robotic system. 2010 Annual International Conference of the IEEE Engineering in Medicine and Biology. https://doi.org/10.1109/iembs.2010.5627930

Vertongen, J., & Kamper, D. (2020b). Design of a 3D printed hybrid mechanical structure for a hand exoskeleton. Current Directions in Biomedical Engineering, 6(2). https://doi.org/10.1515/cdbme-2020-2003

Wang, L., Meydan, T., & Williams, P. (2017, April 5). A Two-Axis Goniometric Sensor for Tracking Finger Motion. Sensors, 17(4), 770. https://doi.org/10.3390/s17040770

Wang, Z., Wang, D., Zhang, Y., Liu, J., Wen, L., Xu, W., & Zhang, Y. (2020). A Three-Fingered Force Feedback Glove Using Fiber-Reinforced Soft Bending Actuators. IEEE Transactions on Industrial Electronics, 67(9), 7681–7690. https://doi.org/10.1109/tie.2019.2924860

Yang, J., Xie, H., & Shi, J. (2016, May). A novel motion-coupling design for a jointless tendon-driven finger exoskeleton for rehabilitation. Mechanism and Machine Theory, 99, 83–102. https://doi.org/10.1016/j.mechmachtheory.2015.12.010